

# Effect of Bending on Critical Current and n-Value of React-and-Jacket Processed Nb<sub>3</sub>Sn Conductor<sup>\*)</sup>

Kazuya TAKAHATA, Hitoshi TAMURA, Toshiyuki MITO, Shinsaku IMAGAWA and Akio SAGARA

National Institute for Fusion Science, 322-6 Oroshi-cho, Toki 509-5292, Japan

(Received 21 November 2012 / Accepted 22 January 2013)

A “react-and-jacket” processed Nb<sub>3</sub>Sn conductor consisting of a Rutherford cable and aluminum-alloy jacket has been developed for fusion magnets. This study investigates the effect of bending on the critical current and the n-value of this conductor, which has a cross-section of  $17 \times 4.9 \text{ mm}^2$ . The conductor was wound in a three-turn coil and its critical current was measured in a superconducting magnet. The degradation of the critical current and the n-value due to the bending strain were assessed using an empirical formula for the strain dependence.

© 2013 The Japan Society of Plasma Science and Nuclear Fusion Research

Keywords: Nb<sub>3</sub>Sn conductor, Rutherford cable, critical current, n-value, bending strain

DOI: 10.1585/pfr.8.2405008

## 1. Introduction

A new large-scale Nb<sub>3</sub>Sn conductor has been developed that includes a Rutherford cable and an aluminum-alloy jacket to support electromagnetic force [1–4]. The manufacturing process of the conductor is unique in that the jacketing process is performed after reaction heat treatment of the Nb<sub>3</sub>Sn Rutherford cable. This process, which we term the “react-and-jacket” process, gives the conductor a high critical current ( $I_c$ ) because the compressive strain induced in the Nb<sub>3</sub>Sn filaments due to the thermal contraction of the jacket material is reduced.  $I_c$  measurements using a short, straight sample have demonstrated that the react-and-jacket process improves the  $I_c$  properties [1]. Using a Rutherford cable is also attractive because

its simple configuration gives a uniform current distribution and high current density in the cable.

This react-and-jacket processed conductor can be wound after the reaction heat treatment to form a magnet. This manufacturing process, the so-called “react-and-wind” process, is more attractive than the conventional wind-and-react process used to fabricate large magnets (e.g., fusion magnets) with Nb<sub>3</sub>Sn superconductors because it does not require a large furnace for the reaction heat treatment. However, the bending strain due to winding should be carefully controlled to prevent degrading  $I_c$  because Nb<sub>3</sub>Sn is a strain-sensitive material.

This paper reports  $I_c$  measurements of a three-turn coil made by the react-and-wind process and discusses the degradation of  $I_c$  and n-value by the bending strain.

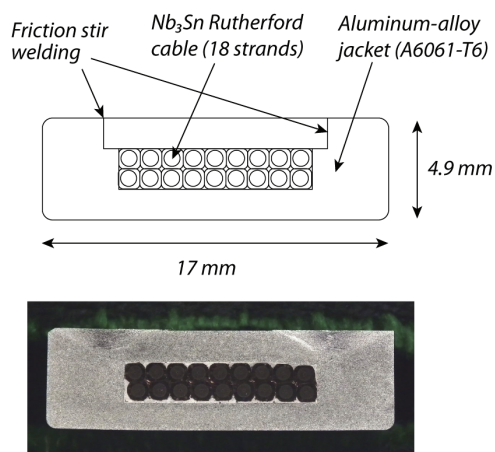


Fig. 1 Schematic diagram and photograph of conductor cross-section.

## 2. Conductor

Figure 1 shows a schematic diagram and a photograph of a cross section of the conductor. Table 1 lists its specifications. The Rutherford cable consists of 18 bronze-route

Table 1 Conductor specifications.

Strands	
Superconductor	Nb <sub>3</sub> Sn
Diameter	1.0 mm
Copper ratio	1.0
Filament diameter	3.7 μm
Twist pitch	25 mm
Conductor	
Dimensions	17.0 × 4.9 mm <sup>2</sup>
Number of strands	18
Cabling pitch	94 mm
Jacket material	Aluminum-alloy 6061-T6
Filler material	Indium

author's e-mail: takahata@LHD.nifs.ac.jp

<sup>\*)</sup> This article is based on the presentation at the 22nd International Toki Conference (ITC22).

$\text{Nb}_3\text{Sn}$  wires with diameters of 1.0 mm. The heat-treated cable and indium sheets as fillers were embedded in the grooved aluminum-alloy jacket. The jacket cover was then welded by friction stir welding [4,5], which does not damage the cable. The  $I_c$  of the straight conductor was measured to be approximately 11 kA at 7 T and 9 kA at 8 T [1].

### 3. Critical Current Measurements

A 3-m-long conductor sample was fabricated and wound flatwise in a three-turn coil (see Fig. 2). The coil had an inner radius of 150 mm. It was inserted into a split superconducting magnet and  $I_c$  was measured under external magnetic fields of 6.3 to 7.1 T. The bath temperature was 4.32 K. The sample current ( $I$ ) was injected by a DC power supply with a sweep rate of 50 A/s. The electric fields ( $E$ ) were then measured by a voltage tap pair including the second turn, which has a length of 1 m. Figure 3 shows the measured electric field as a function of the current at different external magnetic fields. The critical current was determined by the electric field criterion,  $E_c$ . The product of  $I_c$  at 7 T for a single strand and the

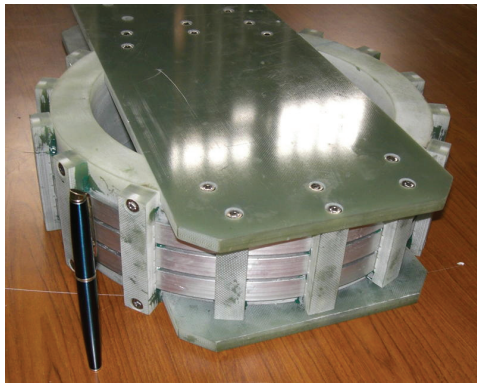


Fig. 2 Photograph of three-turn winding sample for  $I_c$  measurements.

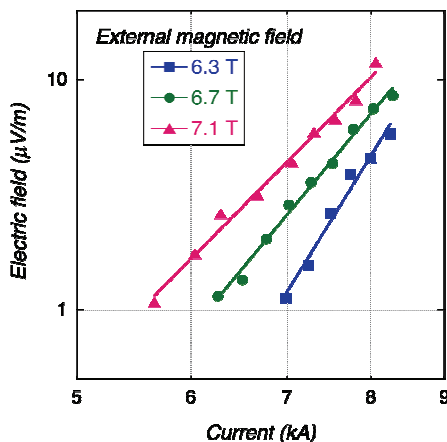


Fig. 3 Measured electric fields versus current at various external magnetic fields for the winding sample of the react-and-jacket processed  $\text{Nb}_3\text{Sn}$  conductor.

number of strands (= 18) was 11 kA. The  $I_c$  of the wound conductor was 8 kA at 7.1 T for the usual criterion  $E_c = 10 \mu\text{V/m}$ . Therefore, the  $I_c$  degradation was found to be 27%. Because the  $I_c$  degradation of a straight conductor was 9% [1], these results show additional  $I_c$  degradation by bending.

The electric field can be expressed by the conventional power-law relation:

$$E = E_c(I/I_c)^n, \quad (1)$$

where  $n$  is the ‘n-value’. The n-value is determined by fitting the measured electric fields, as shown in Fig. 3. The n-value of a single strand is 37 at 7 T. The measured n-value of the wound conductor was 6.3 at 7.1 T, which was reduced to one-sixth of the n-value of a single strand. This means that a strict electric field criterion gives a much lower  $I_c$ . The  $I_c$  was reduced to 5.5 kA at 7.1 T with the strict criterion  $E_c = 1 \mu\text{V/m}$ . In the next section, we will discuss the degradation of  $I_c$  and the n-value due to bending.

### 4. Estimation of Critical Current Degradation

The intrinsic strain in the  $\text{Nb}_3\text{Sn}$  filaments  $\varepsilon$  was estimated using:

$$\varepsilon = \varepsilon_{\text{th}} + \varepsilon_{\text{b}}, \quad (2)$$

where  $\varepsilon_{\text{th}}$  is the thermal strain and  $\varepsilon_{\text{b}}$  is the bending strain. The thermal strain at 4 K was estimated to be  $-0.43\%$  (compression), as described in a previous study [1]. (The aluminum-alloy jacket becomes plastic, rather than elastic, on bending. This transition probably affects the thermal strain generated by cooling from room temperature to cryogenic temperature. While this effect is considered to be small, it will be investigated in future work.) The bending strain is different at different points on the cable. With the bending neutral axis defined as the midline, as shown in Fig. 4, the bending strain depends only on the distance  $y$  according to:

$$\varepsilon_{\text{b}} = y/r_{\text{b}}, \quad (3)$$

where  $r_{\text{b}}$  is the bending radius (152.5 mm for the coil). The maximum bending strains in the filament bundle are estimated to be  $+0.56\%$  (tension) at  $y = +0.854$  mm and  $-0.56\%$  (compression) at  $y = -0.854$  mm. Because the thermal strain  $\varepsilon_{\text{th}}$  is compressive, the intrinsic strain in the inner strands (compression side) is more severe than that in the outer strands (tension side). The most severe intrinsic strain is estimated to be  $-0.99\%$  (compression) at  $y = -0.854$  mm. Therefore, the  $I_c$  degradation is probably determined by the  $I_c$  of the inner strands.

The  $I_c$  of the bent strand can be calculated by integrating the critical current density depending on the intrinsic strain and magnetic field  $J_c(\varepsilon, B)$  over the cross-section

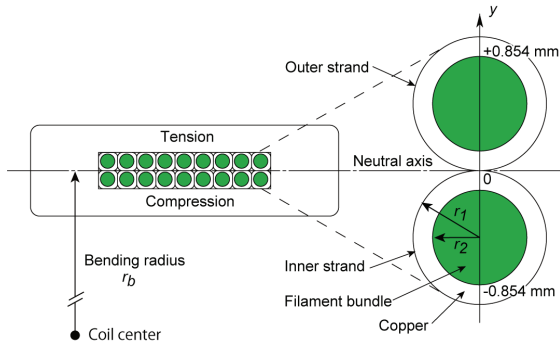


Fig. 4 Schematic of the conductor showing the neutral axis and definition of radii  $r_1$  and  $r_2$ .

of the filament bundle. In previous works, two extreme cases have been considered depending on whether currents can transfer between superconducting filaments [6]. In the case where a current can transfer between filaments without electric fields (called ‘perfect current transfer’),  $I_c$  for a single strand will be equal to the integral of the critical current density over the filament bundle region [6, 7]:

$$I_c = 2 \int_{-r_1-r_2}^{-r_1+r_2} J_c(\varepsilon, B) \sqrt{r_2^2 - (y+r_1)^2} dy, \quad (4)$$

where  $r_1$  and  $r_2$  are the radii of a strand and the filament bundle region, respectively (see Fig. 4). For the strain dependence of the critical current density, we used the empirical formula proposed by Godeke *et al.* [8]. The fitting parameters in the formula were also obtained from their studies, which deal with a similar bronze-route wire made by the same manufacture [8]. (Strictly speaking, the parameters may differ slightly from those for the wire used here.) The magnetic field is the sum of the external magnetic field and the self-magnetic field depending on position and current.

In the case where no current can transfer between filaments due to high resistivity between the filaments (called ‘no current transfer’), the critical current of each filament will be determined by  $J_c$  at its most highly strained point. Because the filaments are twisted in a strand,  $J_c$  will be distributed concentrically. The most highly strained points are located on the  $y$ -axis from the center of the strand  $y = -0.5$  mm to  $y = -0.854$  mm. Therefore,  $I_c$  for a single strand will correspond to the integral of  $J_c$  of the concentric rings [6, 7]:

$$I_c = -2\pi \int_{-r_1-r_2}^{-r_1} J_c(\varepsilon, B)(y+r_1) dy. \quad (5)$$

Figure 5 shows the calculated  $J_c$  distribution in the filament bundle under the assumptions of perfect current transfer and no current transfer at 7.1 T.  $J_c$  is normalized by its maximum value at  $\varepsilon = 0$ . The calculation shows that the no current transfer case is much more severe. The integral of the  $J_c$  distribution then gives  $I_c$ .

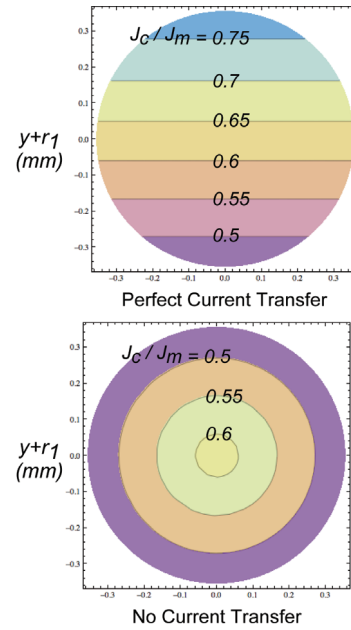


Fig. 5 Calculated  $J_c$  distribution in the filament bundle of the inner strand under the assumptions of perfect current transfer and no current transfer.

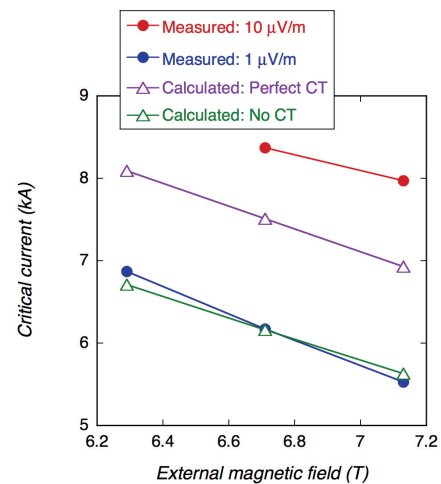


Fig. 6 Comparison between the measured and calculated  $I_c$ .  $I_c$  is calculated under the assumptions of perfect current transfer (CT) and no current transfer.

Figure 6 summarizes the calculated and measured  $I_c$  as a function of the external magnetic field. The results clarify that the calculated  $I_c$  with no current transfer is consistent with the measured  $I_c$  with the strict criterion  $E_c = 1$  μV/m. This can be explained simply by the fact that the no current transfer case indicates the limitations of zero resistivity or perfect superconductivity. In contrast, the perfect current transfer case allows a certain level of electric field due to resistive currents between filaments, although the filaments maintain superconductivity. The degradation of the  $n$ -value can also be explained by a gradual shift of the current distribution from the no current transfer case

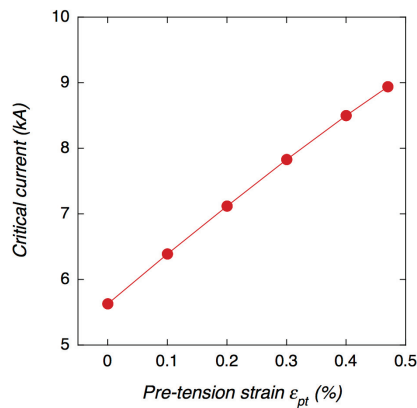


Fig. 7 Improvement of critical current at 7.1 T by pre-tension strain calculated with no current transfer assumption.

to the perfect current transfer case, as shown in Fig. 5. When considering actual magnet applications, the no current transfer assumption would provide a secure conductor design even though it exhibits a lower  $I_c$ , because the electric field of  $1 \mu\text{V}/\text{m}$  will generate a Joule heat of  $100 \text{ W}/\text{m}^3$  in the conductor with a current density of  $10^8 \text{ A}/\text{m}^2$ , which is of the same order of magnitude as nuclear heating in fusion magnets [2].

## 5. Application of Pre-Tension Process

The react-and-jacket processed conductor has the advantage that the strain can be controlled by pre-tensioning of the Rutherford cable. In fact, the pre-tension can be applied to the cable while covering and welding the aluminum-alloy jacket. Here we estimate the improvement of  $I_c$  by pre-tension strain,  $\epsilon_{pt}$ . The intrinsic strain can be written as:

$$\epsilon = \epsilon_{th} + \epsilon_b + \epsilon_{pt}. \quad (6)$$

The tensile strain is limited by the irreversible strain where filament breakage occurs. Godeke *et al.* demonstrated reversibility of the strain dependency up to 0.6% for a similar bronze-route strand made by the same manufacture [9]. Here the irreversible strain is assumed to be 0.6%. (Measurements of the irreversible strain will be necessary for practical applications.) Therefore the maximum pre-tension strain is limited to 0.47%. Figure 7 shows the

calculated  $I_c$  at 7.1 T with no current transfer using (5). The pre-tension is found to improve  $I_c$  substantially.  $I_c$  increases to 9 kA with a pre-tension strain of 0.47%, and the  $I_c$  degradation can be reduced to 18%. Conductors in magnets are also subject to hoop strain by the electromagnetic force. The precise estimation of all possible strains should allow  $I_c$  of the conductor to be maximized.

## 6. Conclusions

$I_c$  measurements of a coil-shaped react-and-jacket processed  $\text{Nb}_3\text{Sn}$  conductor revealed the degradation of  $I_c$  and the n-value due to bending strain. With a strict electric field criterion, such as  $1 \mu\text{V}/\text{m}$ ,  $I_c$  can be calculated using the assumption that no current can transfer between filaments and assuming a distribution of the bending strain. When the current increases from the value of  $I_c$  with a strict electric field criterion, current transfer between filaments occurs and the current distribution shifts while the filaments maintain superconductivity. It is likely that the gradual electric field generation due to the resistive current transfer decreases the n-value. When the conductor is to be used in fusion magnets, a pre-tension process is useful for reducing the  $I_c$  degradation.

## Acknowledgements

The authors would like to express their gratitude to Furukawa Electric Co. Ltd. and Furukawa-Sky Aluminum Corp. for manufacturing the conductor. This work was funded by a grant (No. NIFS12UFAA003) from the Ministry of Education, Culture, Sports, Science and Technology (MEXT) of Japan.

- [1] K. Takahata *et al.*, *Cryogenics* **51**, 397 (2011).
- [2] K. Takahata *et al.*, *Fusion Eng. Des.* **82**, 1487 (2007).
- [3] H. Tamura *et al.*, *Plasma Fusion Res.* **5**, S1035 (2010).
- [4] M. Sugimoto *et al.*, *IEEE Trans. Appl. Super.* **22**, 4802905 (2012).
- [5] C.J. Dawes and W.M. Thomas, *Weld. J.* **75**, 41 (1996).
- [6] M. Takayasu *et al.*, *Supercond. Sci. Technol.* **24**, 045012 (2011).
- [7] J.W. Ekin, *Filamentary A15 Superconductors* (Plenum Press, New York, 1980) p.187.
- [8] A. Godeke *et al.*, *Supercond. Sci. Technol.* **19**, R100 (2006).
- [9] A. Godeke *et al.*, *Rev. Sci. Instrum.* **75**, 5112 (2004).